J. Phys. Chem. A **2005,** *109,* 4939−4949

BAC-MP4 Predictions of Thermochemistry for Gas-Phase Tin Compounds in the Sn−H−C−Cl System

Mark D. Allendorf*

Sandia National Laboratories, Combustion Research Facility, Livermore, California 94551-0969

Carl F. Melius[†]

Lawrence Livermore National Laboratory, Livermore, California 94550

Received: September 23, 2004

In this work, the BAC-MP4 method is extended for the first time to compounds in the fourth row of the periodic table, resulting in a self-consistent set of thermochemical data for 56 tin-containing molecules in the Sn−H−C−Cl system. The BAC-MP4 method combines ab initio electronic structure calculations with empirical corrections to obtain accurate heats of formation. To obtain electronic energies for tin-containing species, the standard 6-31G(d,p) basis set used in BAC-MP4 calculations is augmented with a relativistic effective core potential to describe the electronic structure of the tin atom. Both stable compounds and radical species are included in this study. Trends within homologous series and calculated bond dissociation energies are consistent with previous BAC-MP4 predictions for group 14 compounds and the limited data available from the literature, indicating that the method is performing well for these compounds.

I. Introduction

Tin oxide thin films deposited by chemical vapor deposition (CVD) methods are used extensively in the production of low-emissivity glass, solar cells, flat-panel displays, and gas sensors. Like many industrially important processes, however, the chemistry of tin oxide CVD is rather poorly understood. Organometallic precursors, such as tetramethyl tin ($Sn(CH_3)_4$), monobutyltintrichloride ($C_4H_9SnCl_3$), and dimethyltindichloride ($Sn(CH_3)_2Cl_2$), are often used to make these films. Although the state of tin thermochemistry is, somewhat surprisingly, better than that of the related germanium compounds (see the review by Simoes, Liebman, and Slayden,[1] referred to here as SLS, and the critical review by Gurvich et al.[2]), data for many species relevant to CVD and other high-temperature processes are unavailable. In particular, there are almost no data for halogenated organotin compounds, and data for potential high-temperature intermediates are even more scarce.

Quantum chemistry methods have been previously used to explore the structure and bonding of tin-containing systems; a thorough review of this and other work pertaining to group 14 elements Si, Ge, Sn, and Pb has been published.[3] However, very few investigations focused on gas-phase molecular thermochemistry can be found. An extensive review of the bonding in group 14 compounds is available that includes bond lengths and energies for a number of small tin-containing species.[4] This review also provides a comparison of bond energies predicted by perturbation theory, coupled-cluster calculations, and DFT methods in SnH_3-Y compounds, where Y is a broad range of both organic and inorganic ligands. More recently, we examined the thermochemistry of potential gas-phase reaction pathways occurring during CVD of tin oxide from organometallic precursors, using BAC-MP4 (bond additivity correction method, fourth-order Møller−Plesset perturbation theory) predictions to fill gaps in the thermochemistry.[5,6] Because of their potential importance as reactive intermediates in the oxidation of CVD precursors, we also performed coupled-cluster calculations for the key Sn−O species SnO, SnO_2, H_2SnO, and SnH_4, providing the foundation for predicting the thermochemistry for a wide range of Sn−O compounds.[7]

In this paper, we present a complete description of the application of the BAC-MP4 method to compounds of tin and report the resulting thermochemistry for 56 monomeric compounds in the Sn−H−C−Cl system. The BAC-MP4 method has been used extensively by us and others to predict the thermochemistry for main-group compounds, including compounds of boron,[8] silicon,[9−17] and phosphorus,[18] as well as halogenated hydrocarbons[19−21] and hydrocarbon intermediates.[22] In general, the method yields heats of formation that are in good agreement with established literature values. To obtain the results reported here, a modified version of the BAC-MP4 method was developed in which a relativistic effective core potential (ECP) to describe the electronic structure of the tin atom is used in conjunction with the standard 6-31G(d,p) basis set for lighter main-group elements. Heats of formation, entropies, and free energies of formation are reported for all species included in the investigation. Complete details of the calculations, including polynomial fits suitable for use with the CHEMKIN suite of reacting-flow codes, are available on the web.[23] Although the primary objective is the provision of accurate thermodynamic data, we also briefly describe aspects of the structure and bonding in these compounds that provide insight into tin chemistry.

II. Theoretical Methods

The basic aspects of the standard BAC-MP4 method used here are described in detail in earlier works,[15,22] so we present only a short description here. Electronic structure calculations

---

* Corresponding author. E-mail: mdallen@sandia.gov.

[†] E-mail: melius1@llnl.gov.

10.1021/jp040625+ CCC: $30.25

were performed using Gaussian 98.[24] Because the element tin is not included in the standard basis sets used by the BAC-MP4 method, we employed the relativistic effective core potential (ECP) of LaJohn et al.,[25] in which the core consists of the 1s−4p electrons and the valence $4d^{10}5s^25p^2$ electrons are modeled with an uncontracted Gaussian basis set containing 3s, 3p, and 4d functions (denoted CRENBL and obtained on line from the EMSL Gaussian Basis Set Database[26]). The 6-31G(d) basis set was used for H, C, and Cl to determine equilibrium geometries and harmonic vibrational frequencies, which were obtained at the Hartree−Fock (HF) level of theory. Restricted HF theory (RHF) was applied to the closed-shell molecules, and unrestricted HF theory (UHF) was applied to the open-shell molecules. Vibrational frequencies calculated at this level of theory are known to be systematically larger than experimental values, thus each calculated frequency was scaled by dividing it by 1.12.

To determine atomization enthalpies and thus heats of formation, the effects of electron correlation are included by performing single-point calculations using Møller−Plesset perturbation theory and the HF/6-31G(d) geometries. MP4-(SDTQ)/6-31G(d,p) calculations (fourth-order perturbation theory using the 6-31G(d,p) basis set with single, double, triple, and quadruple substitutions) were performed to obtain electronic energies. This level of theory has been used in most of our previous work, and we find that the errors remaining in the total energies are sufficiently systematic that empirical bond additivity corrections can provide heats of formation accurate to a few kcal mol^{-1}. The form of BAC parameters α_{ij}, A_{ij}, and B_k used to calculate the corrections for individual molecules is given in eqs 1−4 using the example of a bond between atoms X_i and X_j in a molecule of the form $X_k{-}X_i{-}X_j$:

$$E_{\text{BAC}}(X_i - X_j) = f_{ij} g_{kij} \quad (1)$$

where

$$f_{ij} = A_{ij} \exp(-\alpha_{ij} R_{ij}) \quad (2)$$

$$g_{kij} = (1. - h_{ik} h_{ij}) \quad (3)$$

$$h_{ik} = B_k \exp\{-\alpha_{ik}(R_{ik} - 1.4\ \text{Å})\} \quad (4)$$

A_{ij} and α_{ij} are empirically derived parameters that depend on the $X_i{-}X_j$ bond type, and R_{ij} is the bond distance (angstroms). The factor B_k in eq 4 is used to derive a correction for the effects of neighboring atoms on the $X_i{-}X_j$ bond (eq 3) and depends on the identity of atom k. Corrections for UHF instability (singlets) and spin contamination (nonzero ground-state spin) are also applied; the form of these is also described elsewhere.[15]

Table 1 lists the parameters A_{ij}, α_{ij}, and B_k used in this work for each bond type. Corrections for C−C and C−H bonds were established previously.[22] The parameters required to determine BACs for bonds to tin were established by fitting the results of the BAC-MP4(SDTQ) model to established heats of formation available in the literature. The molecules whose heats of formation were used are as follows: Sn−H bonds, SnH_4; Sn−Cl bonds, $SnCl_4$; and Sn−C bonds, $Sn(CH_3)_4$. For Sn−H bonds, the heat of formation for SnH_4 reported by Wagman et al.[27] (38.91 kcal mol^{-1}) is used. The source of this value is unclear, but it appears to be the one adopted by SLS in their review, for which they provide an uncertainty of ±0.5 kcal mol^{-1}. In the case of Sn−Cl bonds, the situation is, somewhat surprisingly, no clearer. We adopted the heat of formation for $SnCl_4$ reported by Gurvich et al. (−114.0 ± 0.5 kcal mol^{-1}) in their critical review because the BAC derived from it yields a good fit to the reported[1] heats of formation in the series $Sn(CH_3)_nCl_{4-n}$. However, other values (some of which are less well documented or without error estimates) can be found in the literature. For example, Wagman et al. report a value of −112.7 kcal mol^{-1} but do not provide the source; Knacke et al. report a value of −120.9 kcal mol^{-1}. The heat of formation of $Sn(CH_3)_4$ appears to be the most firmly established of the three. We adopted the value reported by SLS (−4.85 ± 0.45 kcal mol^{-1}), which is derived from static bomb combustion calorimetry (SBC) measurements, a technique that is considered to be reliable.

TABLE 1: BAC Parameters for the BAC-MP4 (SDTQ) Level of Theory

bond	A_{ij}(MP4)[a]	α_{ij}(MP4)[b]
Sn−H	147.39	2.0
Sn−C	472.71	2.0
Sn−Cl	951.85	2.0
C−H	38.61	2.0
C−C	1444.09	3.8
atom	**B_k(MP4)**	**E[c]**
Sn	0.30	−68.2232532
H	0.00	−0.4982320
C	0.31	−37.7508008
Cl	0.42	−459.5702737

[a] In kcal mol^{-1}. [b] In Å^{-1}. [c] hartree.

Table 2 lists calculated bond lengths for each species as well as the MP4(SDTQ) BACs corresponding to each bond in the molecule and any spin or UHF-instability corrections. The sum of the BACs is combined with the MP4(SDTQ) electronic energy and the unscaled zero-point energy to obtain the heats of atomization and formation at 0 K (ΣD_o and $\Delta H°_f$ (0 K), respectively). Values of the atomic heats of formation at 0 K used in this calculation are given in Table 3 and were obtained from the JANAF Thermochemical Tables,[28] with the exception of tin, the value of which is obtained from Gurvich et al.[2] Entropies, heat capacities, enthalpies, and free energies as a function of temperature were calculated using the heats of formation at 0 K, equations derived from statistical mechanics, and the calculated geometries and scaled frequencies. For consistency with earlier papers in this series, the unscaled frequencies are used for determining the zero-point energy and $\Delta H°_f$ (0 K), whereas the scaled frequencies are used to calculate the thermochemistry at higher temperatures. Minor differences that would result from using the scaled frequencies to calculate $\Delta H°_f$ (0) are incorporated into the BACs. Contributions to the heat capacity and entropy from rotating groups are accounted for by substituting a hindered rotor for the corresponding vibrational frequency determined by the HF calculation,[29] using the interpolation formulas derived by Pitzer and Gwinn.[30] The barrier to rotation is determined from the formula reported by Benson[31] for a torsional vibration, modified so that it yields the barrier reported for the internal rotor in ethane[2] (2.9 kcal mol^{-1}):

$$V_0 = I_{\text{red}} \left(\frac{\nu}{134n} \right)^2 \quad (5)$$

in which V_0 is the barrier height in kcal mol^{-1}, I_{red} is the reduced moment of inertia in amu Bohr,[2] ν is the frequency of the internal rotor in cm^{-1}, and n is the rotational symmetry number of the rotating group. A rotational symmetry number of 3 is assigned to CH_3 groups; all other rotating groups are assigned a value of 2.

There are two major sources of uncertainty in the calculated heats of formation: (1) uncertainties resulting from the ap-

TABLE 2: Bond Additivity Corrections for the MP4(SDTQ) Level of Theory (kcal mol^{-1})

species	spin- or UHF-unstable correction[a]	Sn−H bond length[b] (no.)[c]	BAC	Sn−C bond length (no.)	BAC	Sn−Cl bond length (no.)	BAC	C−H bond length (no.)	BAC	C−C bond length (no.)	BAC
SnH_4		1.713(4)	4.79								
SnH_3CH_3		1.718(3)	4.75	2.161	6.28			1.084(3)	4.42		
SnH_3CH_2	0.88 s	1.715(2)	4.77	2.129	6.69			1.077(2)	4.48		
		1.717	4.75								
$SnH_2(CH_3)_2$		1.722(2)	4.70	2.164(2)	6.21			1.084(2)	4.42		
								1.084(4)	4.41		
$SnH(CH_3)_3$		1.727	4.66	2.167(3)	6.15			1.085(9)	4.41		
$Sn(CH_3)_4$				2.169(4)	6.09			1.085(12)	4.41		
$C_2H_5SnH_3$		1.719	4.74	2.171	6.07			1.085(2)	4.40	1.533	4.21
		1.719(2)	4.73					1.087	4.39		
								1.086(2)	4.40		
$H_2Sn(C_2H_5)_2$		1.725	4.68	2.175(2)	6.00			1.086(8)	4.40	1.534	4.20
		1.725	4.67					1.087(2)	4.39	1.533	4.21
n-$C_3H_7SnH_3$		1.718	4.74	2.170	6.09			1.087(2)	4.39	1.534	4.04
		1.719(2)	4.74					1.087(2)	4.40	1.530	4.16
								1.086(3)	4.40		
i-$C_3H_7SnH_3$		1.719(2)	4.73	2.184	5.86			1.087(3)	4.39	1.533(2)	4.06
		1.720	4.73					1.089(2)	4.38		
								1.086(2)	4.40		
n-$C_4H_9SnH_3$		1.719(3)	4.74	2.170	6.09			1.088(4)	4.38	1.532	3.99
								1.086(5)	4.40	1.529	4.18
										1.534	4.05
SnH_3	0.18 s	1.719(3)	4.74								
SnH_2CH_3	0.16 s	1.726(2)	4.67	2.174	6.12			1.083(2)	4.43		
								1.084	4.42		
$SnH(CH_3)_2$	0.15 s	1.733	4.60	2.178(2)	6.03			1.083(2)	4.42		
								1.084(2)	4.42		
								1.085(2)	4.41		
$Sn(CH_3)_3$	0.15 s			2.182(3)	5.96			1.084(6)	4.42		
								1.086(3)	4.40		
H_3SnCH triplet, trans	1.11	1.715(2)	4.78	2.113	6.19			1.076	4.49		
		1.711	4.81								
H_2SnCH_2	5.99 u	1.70(2)	4.92	1.946	9.64			1.074(2)	4.50		
SnH_2 $^1A_1$	1.60 u	1.774(2)	4.24								
SnH_2 $^3B_1$	0.21 s	1.711(2)	4.81								
$HSnCH_3$ singlet	1.62 u	1.781	4.18	2.210	5.69			1.084	4.42		
								1.087(2)	4.39		
$HSnCH_3$ triplet	0.22 s	1.720	4.73	2.188	5.95			1.082(3)	4.44		
$Sn(CH_3)_2$ singlet	1.50 u			2.214(2)	5.63			1.084(2)	4.41		
								1.088(4)	4.38		
$Sn(CH_3)_2$ triplet	0.21 s			2.193(2)	5.86			1.082(2)	4.43		
								1.083(4)	4.43		
SnH doublet	0.34 s	1.782	4.18								
$SnCH_3$ doublet	0.35 s			2.222	5.55			1.090	4.37		
								1.085(2)	4.41		
SnH_3Cl		1.703(3)	4.89			2.365	8.41				
SnH_2Cl_2		1.695(2)	4.97			2.342(2)	8.76				
$SnHCl_3$		1.689	5.03			2.322(3)	9.08				
$SnCl_4$						2.306(4)	9.32				
$ClSn(CH_3)_3$				2.153(3)	6.29	2.395	7.82	1.084(6)	4.42		
								1.085(3)	4.41		
$Cl_2Sn(CH_3)_2$				2.139(2)	6.47	2.363(2)	8.34	1.082(2)	4.43		
								1.083(4)	4.42		
$Cl_2Sn(CH_3)CH_2$	0.85 s			2.137	6.49	2.357	8.43	1.082	4.43		
				2.107	6.88	2.360	8.38	1.083	4.43		
								1.083	4.42		
								1.076(2)	4.49		
Cl_3SnCH_3				2.131	6.57	2.332(3)	8.86	1.082(3)	4.43		
Cl_3SnCH_2	0.88 s			2.096	7.04	2.237(2)	8.95	1.075(2)	4.50		
						2.328	8.92				
$SnClH_2(CH_3)$		1.708(2)	4.84	2.147	6.43	2.376	8.19	1.084	4.42		
								1.083(2)	4.43		
$SnCl_2H(CH_3)$		1.699	4.93	2.136	6.54	2.352	8.54	1.083(2)	4.43		
								1.082	4.43		
$C_2H_5SnCl_3$				2.146	6.29	2.334	8.82	1.084(4)	4.42	1.532	4.22
						2.336(2)	8.79	1.085	4.41		
n-$C_3H_7SnCl_3$				2.145	6.31	2.335	8.80	1.086(4)	4.40	1.535	4.04
						2.336(2)	8.78	1.085(3)	4.41	1.530	4.16
i-$C_3H_7SnC_3$				2.164	6.00	2.338(2)	8.75	1.085(3)	4.41	1.532(2)	4.07
						2.339	8.73	1.087(2)	4.39		
								1.084(2)	4.41		

TABLE 2 (Continued)

species	spin- or UHF-unstable correction[a]	Sn−H bond length[b] (no.)[c]	BAC	Sn−C bond length (no.)	BAC	Sn−Cl bond length (no.)	BAC	C−H bond length (no.)	BAC	C−C bond length (no.)	BAC
n-$C_4H_9SnCl_3$				2.145	6.31	2.335	8.80	1.087(4)	4.39	1.532	3.98
						2.336(2)	8.78	1.085(3)	4.41	1.528	4.19
								1.086(2)	4.40	1.534	4.04
$CH_3CH_2CH_2CHSnCl_3$	0.98 s			2.101	6.87	2.329	8.90	1.086(4)	4.40	1.534	3.93
						2.334	8.82	1.087	4.39	1.528	4.19
						2.332	8.85	1.091	4.36	1.508	4.44
								1.085	4.41		
								1.078	4.47		
$CH_2CH_2CH_2CH_2SnCl_3$	0.75 s			2.145	6.31	2.335	8.81	1.092	4.35	1.535	3.93
						2.336	8.79	1.087	4.39	1.500	4.64
						2.336	8.78	1.086(2)	4.40	1.534	4.05
								1.075	4.50		
								1.076	4.49		
								1.085(2)	4.41		
SnH_2Cl $^2A'$	0.23 s	1.719(2)	4.74			2.377	8.21				
$SnHCl_2$ $^2A'$	0.46 s	1.723	4.70			2.359(2)	8.47				
$SnCl_3$	0.51 s					2.346(3)	8.66				
Cl_2SnCH_3	0.64 s			2.179	6.00	2.374(2)	8.18	1.082(2)	4.44		
								1.083	4.43		
$ClSn(CH_3)_2$	0.31 s			2.172(2)	6.08	2.403	7.73	1.082(2)	4.43		
								1.084(2)	4.42		
								1.084(2)	4.41		
Cl_2SnCH_2	7.84 u			2.028	8.09	2.347(2)	8.63	1.080(2)	4.46		
HSnCl $^1A'$		1.773	4.25			2.413	7.64				
HSnCl $^3A''$	0.44 s	1.720	4.73			2.374	8.24				
$SnCl_2$ $^1A_1$						2.396(2)	7.87				
$SnCl_2$ $^3B_1$	0.49 s					2.361(2)	8.44				
$ClSnCH_3$ singlet				2.196	5.83	2.427	7.40	1.086	4.40		
								1.087(2)	4.39		
$ClSnCH_3$ triplet	0.94 s			2.255	5.18	2.403	7.75	1.079(3)	4.46		
SnCl doublet	0.37 s					2.419	7.54				

[a] u, UHF-unstable correction; s, spin-contamination correction. [b] In angstroms. [c] Number of bonds.

plicability of the theoretical methods to a given molecule and (2) systematic uncertainties resulting from the lack of good reference compounds for the BACs. The magnitude of the first is estimated using an ad hoc method developed previously (eq 6) that uses the results from lower-level calculations[15] and is reported in Table 3.

$$\text{error(BAC-MP4)} = \{1.0\ \text{kcal mol}^{-1} + (\Delta H_{\text{BAC-MP4}} - \Delta H_{\text{BAC-MP3}})^2 + (\Delta H_{\text{BAC-MP4}} - \Delta H_{\text{BAC-MP4SDQ}})^2 + 0.25(E_{\text{BAC}}(\text{spin}_{\text{S}}2)\ \text{or}\ E_{\text{BAC}}(\text{spinUHF-I}))^2\}^{1/2} \quad (6)$$

The second source of uncertainty can add a few kcal mol^{-1} to the uncertainty estimates and scales with the number of bonds in the molecule. The use of different reference values would shift our calculated heats of formation as a group, with the consequence that calculated bond dissociation enthalpies and reaction enthalpies are affected less than the individual heats of formation. Overall, we believe that the uncertainties in the BAC-MP4 heats of formation lie in the ±2−7 kcal mol^{-1} range.

Bond energies at 298 K for most compounds were calculated using the BAC-MP4 results. Heats of formation at the BAC-MP4 level for the polyatomic ligands involved in these reactions are also given in Table 3. When the bound group is an atom, the experimental atomic heat of formation (Table 3) was used to calculate the bond energy.

III. Results and Discussion

The BAC-MP4 calculations described here provide thermodynamic data appropriate for modeling, as well structural data for each of the 56 molecules examined. Because the primary focus of this paper is on thermodynamic properties, we present only the bond lengths and associated BACs (Table 2), as well as heats of formation at various levels of theory (0 K) and at 298 K (Table 3) and the entropy $S°(298)$ and Gibbs free energy of formation $\Delta G°_f(298)$ (Table 4). Additional information, including molecular structures in the form of Cartesian coordinates, moments of inertia, vibrational frequencies, data concerning hindered rotors, and raw electronic energies (in hartrees), is available on the web.[23] Polynomial fits in the format appropriate for use in CHEMKIN[32] calculations, as well as additional details of the ab initio calculations, can also be found there.

Tetravalent Molecules. Five series of closed-shell tetracoordinate molecules are included in this investigation: $Sn(CH_3)_nH_{4-n}$, $SnCl_nH_{4-n}$, $SnCl_n(CH_3)_{4-n}$, SnH_3R, and $SnCl_3R$ ($R = CH_3$, C_2H_5, *n*-C_3H_7, *n*-C_4H_9). In $Sn(CH_3)_nH_{4-n}$, the molecules are very close to tetrahedral, with the maximum deviation from 109.5° of the XSnY bond angles less than 4.5° in all cases. Structural trends with ligand exchange, such as the decrease in both Sn−C and Sn−Cl bond lengths with increasing number of Cl ligands (Table 2), are reproduced by the calculations. (See discussion below.) However, the geometries predicted at the HF/CRENBL-6-31(d) level of theory are somewhat longer than the experimental values. For example, the calculated and experimental[33] (in parentheses) Sn−R bond lengths in SnH_4, $Sn(CH_3)_4$, and $SnCl_4$ are 1.713 (1.711), 2.169 (2.144), and 2.306 Å (2.281 Å), respectively (standard deviations are ±0.005 for the experimental data). Such differences are similar to those predicted for analogous silicon compounds by all-electron calculations using uncorrelated methods and are attributed to

TABLE 3: Calculated Heats of Formation for Sn−H−C−Cl Compounds at Various Levels of Theory (0 K) and at 298 K (with Estimated Error) and Comparison with Published Values (kcal mol^{-1})

species	MP4	BAC-MP2	BAC-MP3	BAC-MP4			literature
				SDQ (0 K)	SDTQ (0 K)	SDTQ (298 K)	
SnH_4	61.0	41.8	41.8	41.8	41.8	38.9 ± 1.0	38.9 ± 0.5[a,f]
SnH_3CH_3	66.4	32.8	32.6	32.6	32.6	28.3 ± 1.0	
SnH_3CH_2	112.9	82.2	81.3	81.3	82.0	78.7 ± 1.5	
$SnH_2(CH_3)_2$	71.4	23.4	23.1	23.0	23.1	17.5 ± 1.0	21.0 ± 1.0[a]
$SnH(CH_3)_3$	75.9	13.6	13.2	13.1	13.1	6.4 ± 1.0	6.0 ± 1.0[a]
$Sn(CH_3)_4$	80.1	3.4	3.1	3.0	2.9	−4.9 ± 1.0	−4.9 ± 1.0[a,f]
$C_2H_5SnH_3$	78.5	31.8	32.3	32.5	32.0	26.2 ± 1.1	
$H_2Sn(C_2H_5)_2$	95.5	21.5	22.6	23.0	21.8	13.5 ± 1.8	
n-$C_3H_7SnH_3$	87.1	27.2	28.2	28.7	27.8	20.5 ± 1.4	
i-$C_3H_7SnH_3$	88.0	28.3	29.8	30.1	29.1	21.8 ± 1.6	
n-$C_4H_9SnH_3$	96.2	23.3	24.6	25.3	24.1	15.4 ± 1.6	
SnH_3	78.1	63.6	63.9	63.8	63.7	61.7 ± 1.0	
SnH_2CH_3	84.1	55.2	55.5	55.2	55.2	51.7 ± 1.0	
$SnH(CH_3)_2$	89.6	46.3	46.7	46.4	46.3	41.5 ± 1.1	
$Sn(CH_3)_3$	94.6	36.9	37.5	37.2	36.9	31.0 ± 1.2	31.1 ± 4.1[a]
H_3SnCH triplet, trans	159.6	132.4	131.4	131.7	132.7	130.2 ± 1.9	
H_2SnCH_2	109.7	76.7	79.2	77.7	75.2	72.6 ± 4.9	
$SnH_2\ {}^1A_1$	69.2	61.1	59.9	59.5	59.2	58.0 ± 1.3	
$SnH_2\ {}^3B_1$	94.3	83.9	84.6	84.5	84.5	83.4 ± 1.0	
$HSnCH_3$ singlet	74.8	51.6	51.2	50.7	50.1	47.4 ± 1.6	
$HSnCH_3$ triplet	101.2	76.6	77.4	77.1	77.0	74.2 ± 1.1	
$Sn(CH_3)_2$ singlet	79.2	41.1	41.4	41.0	40.1	36.2 ± 1.9	
$Sn(CH_3)_2$ triplet	107.9	69.1	70.2	69.8	69.4	65.3 ± 1.3	
SnH doublet	73.4	69.9	69.5	69.1	68.9	68.4 ± 1.2	
$SnCH_3$ doublet	79.2	60.6	61.0	60.6	60.1	58.1 ± 1.5	
SnH_3Cl	26.0	2.4	2.6	2.8	2.9	0.4 ± 1.1	
SnH_2Cl_2	−9.4	−37.5	−37.3	−37.1	−36.8	−38.8 ± 1.1	
$SnHCl_3$	−43.9	−76.6	−76.5	−76.3	−76.1	−77.4 ± 1.1	
$SnCl_4$	−76.7	−114.0	−114.0	−114.0	−114.0	−114.4 ± 1.0	−114.4 0.5[b,f]
$ClSn(CH_3)_3$	33.7	−32.9	−32.9	−32.8	−32.8	−38.7 ± 1.0	−46.4 ± 4[d]
$Cl_2Sn(CH_3)_2$	−8.5	−65.1	−64.9	−64.8	−64.7	−68.8 ± 1.0	−70.9 ± 5[g]
$Cl_2Sn(CH_3)CH_2$	38.8	−14.8	−15.6	−15.3	−14.5	−17.6 ± 1.7	
Cl_3SnCH_3	−45.4	−92.2	−92.0	−91.9	−91.9	−94.1 ± 1.0	−95.7[e]
Cl_3SnCH_2	2.8	−41.1	−41.9	−41.7	−40.9	−42.1 ± 1.6	
$SnClH_2(CH_3)$	28.8	−9.1	−9.1	−9.0	−8.8	−12.6 ± 1.1	
$SnCl_2H(CH_3)$	8.9	51.3	51.1	50.9	50.7	−53.7 ± 1.1	
$Cl_3SnC_2H_5$	−34.8	−94.6	−93.5	−93.1	−93.8	−97.5 ± 1.2	
n-$C_3H_7SnCl_3$	−26.3	−99.3	−97.6	−96.9	−98.0	−103.2 ± 1.6	
i-$C_3H_7SnCl_3$	−26.7	−99.5	−97.0	−96.4	−97.9	−102.9 ± 2.0	
n-$C_4H_9SnCl_3$	−17.4	−103.4	−101.3	−100.4	−101.9	−108.4 ± 1.9	
$CH_3CH_2CH_2CHSnCl_3$	27.3	−55.9	−55.5	−54.6	−54.9	−60.5 ± 1.2	
$CH_2CH_2CH_2CH_2SnCl_3$	28.7	−54.5	−52.8	−51.9	−52.7	−58.0 ± 1.3	
$SnH_2Cl\ {}^2A'$	42.2	23.8	24.3	24.2	24.2	22.5 ± 1.0	
$SnHCl_2\ {}^2A'$	4.6	−18.2	−17.3	−17.3	−17.5	−18.6 ± 1.0	
$SnCl_3$	−32.3	−59.4	−58.2	−58.3	−58.8	−59.2 ± 1.3	−69.9 ± 12[b]
Cl_2SnCH_3	4.6	−32.5	−31.2	−31.3	−31.7	−33.9 ± 1.2	
$ClSn(CH_3)_2$	47.8	0.5	1.4	1.3	1.0	−3.0 ± 1.1	
Cl_2SnCH_2	41.2	2.4	4.3	2.7	−0.9	−2.2 ± 6.6	
$HSnCl\ {}^1A'$	21.8	11.0	10.8	10.7	9.9	9.0 ± 1.5	
$HSnCl\ {}^3A''$	62.5	48.4	49.4	49.2	49.1	48.3 ± 1.0	
$SnCl_2\ {}^1A_1$	−29.1	−44.8	−43.4	−43.6	−44.9	−45.2 ± 2.2	−48.4 ± 1.7[b]
$SnCl_2\ {}^3B_1$	34.1	16.2	17.2	17.0	16.7	16.4 ± 1.2	
$ClSnCH_3$ singlet	24.3	−1.7	−1.0	−1.2	−2.2	−4.3 ± 1.8	
$ClSnCH_3$ triplet	65.2	37.5	38.8	38.4	38.0	35.9 ± 1.4	
$SnCl$ doublet	25.0	17.1	17.9	17.8	17.1	16.8 ± 1.5	34.7 ± 2.9[b]
$Sn({}^3P_0)$	72.3	72.0	72.0	72.0	72.0	72.0 ± 1.0	71.99 ± 0.36[b]
H						52.07[c]	
$C({}^3P)$						171.21[c]	
Cl						28.98[c]	
CH_3						34.9 ± 1.2[h]	
$CH_2({}^3B_1)$						92.8 ± 1.4[h]	
C_2H_5						28.8 ± 1.3[h]	
n-C_3H_7						24.8 ± 1.3[h]	
n-C_4H_9						19.7 ± 1.2[h]	

[a] SLS review.[1] [b] Gurvich et al.[2] [c] JANAF Thermochemical Tables.[28] [d] Reference 47. [e] Average of values cited in ref 48. No error estimate is given; we estimate a minimum of ± 2 kcal mol^{-1}. [f] Reference compound used to establish BAC. [g] Average of values.[49] [h] Reference 22.

finite basis-set size.[34] Thus, they will not significantly affect BAC-MP4 heats of formation because they are systematic in nature and are accounted for by the BAC corrections, which are based on heats of formation that are presumed to be accurate. The literature reveals, somewhat unexpectedly, that better agreement between calculated and observed Sn−Cl and Sn−C

TABLE 4: BAC-MP4 Thermochemical Parameters for Sn−H−C−Cl Compounds at Various Temperatures

	$\Delta H_f^{\circ\,a}$	$S^{\circ\,b}$	$\Delta G_f^{\circ a}$					
species	298 K	298 K	300 K	600 K	1000 K	1500 K	2000 K	2500 K
SnH_4	38.9	54.7	44.8	51.8	62.9	76.6	89.9	102.9
SnH_3CH_3	28.3	68.2	39.9	52.9	72.5	97.2	121.4	145.1
SnH_3CH_2	78.7	71.5	84.7	91.6	102.8	116.8	130.5	143.8
$SnH_2(CH_3)_2$	17.5	79.9	35.3	54.9	83.9	120.5	156.5	191.8
$SnH(CH_3)_3$	6.4	92.1	30.4	56.4	94.4	142.6	190.1	236.7
$Sn(CH_3)_4$	−4.9	102.9	25.6	58.4	106.0	166.4	226.1	284.6
$C_2H_5SnH_3$	26.2	78.9	44.3	64.2	93.6	130.5	166.7	202.1
$H_2Sn(C_2H_5)_2$	13.5	98.9	45.1	79.1	128.0	189.8	250.5	310.0
n-$C_3H_7SnH_3$	20.5	86.5	46.1	73.8	113.7	163.9	213.0	261.0
i-$C_3H_7SnH_3$	21.8	85.9	47.6	75.4	115.5	166.0	215.4	263.8
n-$C_4H_9SnH_3$	15.4	94.2	48.4	83.8	134.5	197.9	260.0	320.5
SnH_3	61.7	57.4	62.2	63.5	67.1	71.7	76.1	80.5
SnH_2CH_3	51.7	70.6	57.9	65.4	77.7	93.6	109.1	124.4
$SnH(CH_3)_2$	41.5	81.6	54.2	68.5	90.4	118.5	146.3	173.5
$Sn(CH_3)_3$	31.0	92.7	50.1	71.2	102.7	143.0	182.8	222.0
H_3SnCH triplet, trans	130.2	69.8	132.0	134.6	139.8	146.3	152.6	158.8
H_2SnCH_2	72.6	65.3	75.7	79.8	87.0	96.3	105.3	114.1
$SnH_2\ {}^1A_1$	58.0	54.8	54.5	51.9	50.1	48.3	46.6	45.0
$SnH_2\ {}^3B_1$	83.4	56.7	79.4	76.1	73.6	70.9	68.3	65.8
$HSnCH_3$ singlet	47.4	67.6	49.9	53.5	60.7	70.3	79.9	89.5
$HSnCH_3$ triplet	74.2	69.5	76.1	79.2	85.7	94.6	103.5	112.3
$Sn(CH_3)_2$ singlet	36.2	80.3	44.6	54.5	70.5	91.5	112.3	132.9
$Sn(CH_3)_2$ triplet	65.3	80.9	73.5	83.3	99.4	120.5	141.5	162.3
SnH doublet	68.4	50.9	61.5	55.2	48.5	40.6	32.9	25.5
$SnCH_3$ doublet	58.1	65.4	56.5	56.0	57.5	60.1	62.9	65.7
SnH_3Cl	0.4	68.5	5.5	11.4	20.9	32.6	43.9	55.0
SnH_2Cl_2	−38.8	75.7	−32.6	−25.7	−15.3	−2.4	10.2	22.5
$SnHCl_3$	−77.4	83.2	−70.1	−62.4	−51.1	−37.2	−23.7	−10.3
$SnCl_4$	−114.4	88.5	−105.4	−96.3	−83.3	−67.3	−51.7	−36.3
$ClSn(CH_3)_3$	−38.7	100.9	−14.1	12.3	50.7	99.3	147.3	194.4
$Cl_2Sn(CH_3)_2$	−68.8	98.6	−50.0	−29.9	−0.6	36.2	72.6	108.3
$Cl_2Sn(CH_3)CH_2$	−17.6	100.2	−3.9	10.7	32.0	59.0	85.6	111.6
Cl_3SnCH_3	−94.1	94.0	−80.4	−65.9	−44.9	−18.7	7.1	32.5
Cl_3SnCH_2	−42.1	97.0	−33.9	−25.3	−12.8	2.8	18.1	33.2
$SnClH_2(CH_3)$	−12.6	79.3	−1.0	11.8	30.9	55.0	78.5	101.7
$SnCl_2H(CH_3)$	−53.7	88.6	−41.6	−28.6	−9.8	13.7	36.6	58.9
$C_2H_5SnCl_3$	−97.5	104.3	−77.0	−55.5	−24.8	13.7	51.6	88.8
n-$C_3H_7SnCl_3$	−103.2	112.1	−75.3	−46.1	−4.8	47.0	98.0	148.1
i-$C_3H_7SnCl_3$	−102.9	111.5	−74.9	−45.6	−4.1	48.0	99.2	149.4
n-$C_4H_9SnCl_3$	−108.4	119.9	−73.2	−36.2	15.8	81.0	144.9	207.2
$CH_3CH_2CH_2CHSnCl_3$	−60.5	123.4	−31.0	0.0	44.0	99.2	153.5	206.6
$CH_2CH_2CH_2CH_2SnCl_3$	−58.0	123.0	−28.3	2.7	46.3	101.0	154.6	206.9
$SnH_2Cl\ {}^2A'$	22.5	68.7	22.9	24.0	27.0	30.9	34.6	38.4
$SnHCl_2\ {}^2A'$	−18.6	77.6	−17.6	−16.1	−12.8	−8.5	−4.4	−0.2
$SnCl_3$	−59.2	84.1	−56.8	−54.2	−49.6	−43.7	−37.9	−32.1
Cl_2SnCH_3	−33.9	88.9	−26.6	−18.4	−5.6	10.8	27.0	43.0
$ClSn(CH_3)_2$	−3.0	90.8	10.2	24.8	47.0	75.4	103.4	131.0
Cl_2SnCH_2	−2.2	85.0	1.6	6.0	13.1	22.2	31.0	39.6
$HSnCl\ {}^1A'$	9.0	65.7	5.6	2.9	0.9	−1.3	−3.3	−5.1
$HSnCl\ {}^3A''$	48.3	67.8	44.2	40.8	37.9	34.6	31.5	28.5
$SnCl_2\ {}^1A_1$	−45.2	73.5	−47.7	−49.7	−50.8	−51.9	−52.8	−53.5
$SnCl_2\ {}^3B_1$	16.4	76.0	13.2	10.5	8.3	6.0	3.9	2.1
$ClSnCH_3$ singlet	−4.3	77.0	−1.4	2.6	10.0	20.0	30.0	40.1
$ClSnCH_3$ triplet	35.9	80.5	37.7	40.6	46.6	54.8	63.1	71.3
SnCl doublet	16.8	60.8	10.2	4.2	−2.3	−10.0	−17.3	−24.4
$Sn(^3P_0)$	72.0	42.4	62.9	54.4	44.5	32.5	20.6	9.0

[a] In kcal mol^{-1}. [b] In cal mol^{-1} K^{-1}.

bond lengths can be achieved for the $SnCl_n(CH_3)_{4-n}$ molecules[35] using the large-core (46-electron) ECP of Wadt and Hay (WH).[36] We have not performed a systematic comparison of CRENBL with WH to determine the reasons for these differences. However, they may be due to a more accurate treatment of scalar relativistic effects in the WH ECP.

All Sn−ligand bond lengths are somewhat affected by substitution within the molecule. The magnitude of these changes is smallest in the series $Sn(CH_3)_nH_{4-n}$, with both Sn−H and Sn−C bonds lengthening only slightly with increasing methyl substitution. In contrast, Cl substitution for CH_3 decreases the length of both Sn−C and Sn−Cl bonds by substantial amounts, in agreement with previously reported results at other levels of theory.[35,37] For example, the Sn−CH_3 bond length decreases from 2.169 Å in $Sn(CH_3)_4$ to 2.131 Å in $SnCl_3(CH_3)_4$, and the Sn−Cl bond length decreases nearly 0.06 Å from $ClSn(CH_3)_3$ to $SnCl_4$. Such effects have been studied extensively and are described variously as hyperconjugation, geminal ligand effects, or the anomeric effect. They are thought to be a consequence of adjacent ligands with interacting σ- and π-donation abilities;[34] for example, CH_3 is both a σ donor and a π donor, whereas Cl is a σ acceptor and a π donor. A detailed discussion of these effects is beyond the scope of this article.

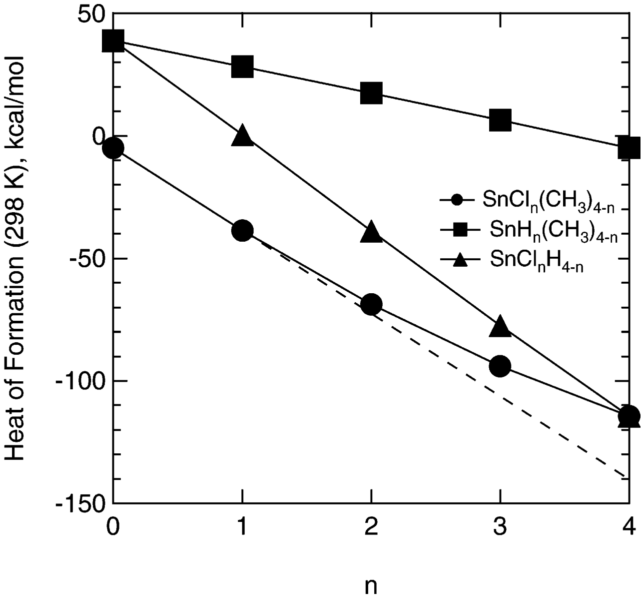

Figure 1. Trends in the heats of formation (298 K) for tetravalent species. The dashed line indicates a linear extrapolation of the first two points in the $SnCl_n(CH_3)_{4-n}$ series, highlighting the nonlinearity of the heats of formation.

However, these structural changes are noteworthy because they correlate with nonlinear trends in the heats of formation for these molecules (Figure 1) and, as will be seen below, with changes in bond energies. Structure−property relationships of this type are not new and have been extensively characterized for group 14 compounds, including those of tin.[38] Of the three ligand-exchange series examined here, the two involving the exchange of hydrogen for either Cl or CH_3 display an essentially linear decrease in the heat of formation as the number of Cl or CH_3 ligands increases. In the case of $Sn(CH_3)_nH_{4-n}$, $\Delta H°$(298 K) decreases uniformly by 11 kcal mol^{-1} with each methyl substitution. The exchange of H by Cl in the series $SnCl_nH_{4-n}$ results in much greater stabilization; $\Delta H°$(298 K) decreases by 38 kcal mol^{-1} for each Cl ligand. Although we have not performed a detailed analysis of the electronic structure, these linear changes are consistent with the explanation that the H ligand has no π-donor capability and thus is not susceptible to the types of interactions described above. This localizes the bonding so that the effects of ligand exchange are essentially additive. In contrast, the differing σ- and π-bonding properties of CH_3 and Cl result in a nonlinear decrease of the heats of formation in the series $SnCl_n(CH_3)_{4-n}$. The largest change (33.8 kcal mol^{-1}) occurs for the first Cl-for-CH_3 substitution, whereas substitution to form $SnCl_4$ stabilizes the molecule by only 20.3 kcal mol^{-1}. As seen in both Figure 1 and Table 3, the BAC-MP4 heats of formation for both the $Sn(CH_3)_nH_{4-n}$ and $SnCl_n(CH_3)_{4-n}$ series are in good agreement with the available experimental data (no data are available for $SnCl_nH_{4-n}$, except for the end members of the series, which are used as reference values, and the BAC-MP4 predictions are thus fixed to the experimental values), confirming the ability of the BAC-MP4 method to reproduce these ligand-interaction effects.

Although BAC-MP4 calculations for the largest alkyl-tin compounds known are impractical, the near-perfect linearity displayed by the heat of formation as a function of the number of methyl groups in the $Sn(CH_3)_nH_{4-n}$ series suggests that heats of formation for larger tin compounds can be accurately predicted by extrapolating the line established by SnH_4 and SnH_3R to larger numbers of R. For example, with R = C_2H_5, n-C_3H_7, and n-C_4H_9 heats of formation for the corresponding SnR_4 compounds of −11.9, −34.7, and −55.1 kcal mol^{-1}, respectively, are obtained. With the exception of R = n-C_4H_9, these values are in very good agreement with the experimental values:[1] −10.8 ± 0.6, −34.9 ± 1.4, and −52.4 ± 1.0 kcal mol^{-1}.

The relatively poor agreement with the $Sn(n\text{-}C_4H_9)_4$ experimental value may be due to the accumulation of error within the BAC-MP4 calculation. However, it appears equally likely that this is the result of experimental error. In fact, our calculations suggest that the conclusion of Simoes et al. in which the measured heat of formation of $Sn(n\text{-}C_4H_9)_4$ is accurate but the value for $Sn(C_2H_5)_4$ is in error[1] is incorrect. Using the same kind of linear analysis described above but plotting instead the heats of formation of SnR_4 for R = C_2H_5, n-C_3H_7, and n-C_4H_9 as a function of the number of carbon atoms in the molecule, Simoes et al. conclude that it is likely that at least one of these heats of formation is inaccurate. However, extending our linear extrapolation for $Sn(C_2H_5)_nH_{4-n}$ by calculating the BAC-MP4 heat of formation for $SnH_2(C_2H_5)_2$, we obtain the same heat of formation for $Sn(C_2H_5)_4$ that results from the line established by only the first two compounds in the series, showing that this series is highly linear. Although Simoes et al. suggest that the liquid enthalpy of formation for $Sn(C_2H_5)_4$ is the source of the error, we believe it more likely that the problem lies with the assumption of linearity among a series of compounds that contain different alkyl chain lengths. Although heats of formation appear to be almost perfectly linear within a given SnR_nH_{4-n} series, this cannot be expected from series that contain different ligands. In other words, the assumption that $\Delta H°_f = \alpha n_C + \beta$, where n_C is the number of carbon atoms, is accurate only for the constant identity of R. A clear illustration of this can be made by comparing the BAC-MP4 heats of formation predicted for $SnH_2(C_2H_5)_2$ and $SnH_3(n\text{-}C_4H_9)$. Although these two compounds contain identical numbers of carbon atoms, their heats of formation (13.5 and 15.4 kcal mol^{-1}, respectively) are significantly different. This example points out the danger of overextending the assumption of localized bonding, even within these relatively simple compounds. Clearly, this assumption cannot be made for compounds in series such as $SnCl_n(CH_3)_{4-n}$, as discussed above.

Bonds to tin in these compounds (Table 5) are much weaker than in the analogous group 14 compounds higher in the periodic table, with Sn−ligand bond energies following the order Sn−Cl $\gg$ Sn−CH_3 $\approx$ Sn−H. For example, Sn−C and Sn−Cl bond energies are 20−27 kcal mol^{-1} lower than for the same bonds in the analogous silicon compounds.[9,10] However, C−H bond energies are largely unchanged from those of hydrocarbons (102−104 kcal mol^{-1}). Tin−chlorine bond strengths are highly dependent on the identity of the other ligands in the molecule, resulting in values as low as 84 kcal mol^{-1} in $SnCl_4$ to 99 kcal mol^{-1} in $SnCl(CH_3)_3$. Sn−H and Sn−CH_3 bonds are less affected by other groups. Sn−H bonds span the relatively narrow range of energies from 70 to 77 kcal mol^{-1}, whereas Sn−CH_3 bonds display an even smaller variability (68−71 kcal mol^{-1}). Increasing the size of the alkyl group has little effect on the Sn−C bond energy. As seen in Table 5, these energies vary by only ±3 kcal mol^{-1} across the series SnH_3R (R = CH_3 to C_4H_9) and even less across the analogous series of chlorinated compounds. The $(CH_3)_3$Sn−H and $(CH_3)_3$Sn−CH_3 bond energies derived by Simoes et al. (77.1 and 71.0 kcal mol^{-1}, respectively) from experiment are in very good agreement with the predicted values for these compounds. However, the Sn−CH_3 bond energy estimated by Johnson and Price from kinetic experiments,[39] 64.5 kcal mol^{-1}, does not agree well with

TABLE 5: Selected BAC-MP4 Bond Energies (298 K, kcal mol^{-1})

		Sn−H Bonds			
SnH_4	74.9	SnH_3	48.4	$HSnCH_3$ singlet	62.8
SnH_3CH_3	75.5	SnH_2CH_3	47.8	$HSnCH_3$ triplet	36
SnH_3CH_2	46	$SnH(CH_3)_2$	46.8	SnH doublet	55.7
$SnH_2(CH_3)_2$	76.1	SnH_2 $^1A_1$	62.5		
$SnH(CH_3)_3$	76.7	SnH_2 triplet	37.1	HSnCl $^1A'$	59.9
SnH_3Cl	74.2	SnH_2Cl $^2A'$	38.6	HSnCl $^3A''$	20.6
SnH_2Cl_2	72.3	$SnHCl_2$ $^2A'$	25.5		
$SnHCl_3$	70.3				
		Sn−C Bonds			
SnH_3CH_3	68.3	n-$C_3H_7SnH_3$	66	H_2SnCH_2	78.2
SnH_3CH_2	17.9	i-$C_3H_7SnH_3$	61.3	SnH_2CH_3	41.2
$SnH_2(CH_3)_2$	69.1	n-$C_4H_9SnH_3$	66.0	$SnH(CH_3)_2$	40.8
$SnH(CH_3)_3$	70	SnH_2CH_3	41.2	$Sn(CH_3)_3$	40.1
$Sn(CH_3)_4$	70.8	$SnH(CH_3)_2$	40.8	H_2SnCH_2	78.2
$C_2H_5SnH_3$	64.3	$Sn(CH_3)_3$	40.1	$HSnCH_3$ singlet	55.9
				$SnCH_3$ doublet	48.8
$ClSn(CH_3)_3$	70.6	$SnClH_2(CH_3)$	70	Cl_2SnCH_3	23.6
$Cl_2Sn(CH_3)_2$	69.8	$C_2H_5SnCl_3$	67.1	$ClSn(CH_3)_2$	33.6
$Cl_2Sn(CH_3)CH_2$	76.5	n-$C_3H_7SnCl_3$	68.8	Cl_2SnCH_2	49.8
Cl_3SnCH_3	69.8	i-$C_3H_7SnCl_3$	65.1	$ClSnCH_3$ singlet	56
Cl_3SnCH_2	75.7	n-$C_4H_9SnCl_3$	68.9	$ClSnCH_3$ triplet	15.8
		Sn−Cl Bonds			
SnH_3Cl	90.3	Cl_3SnCH_2	68.9	HSnCl $^1A'$	88.4
SnH_2Cl_2	90.3	$SnClH_2(CH_3)$	93.3	HSnCl ^3A	49.1
$SnHCl_3$	87.8	SnH_2Cl $^2A'$	64.5	$SnCl_2$ $^1A_1$	91
$SnCl_4$	84.2	$SnHCl_2$ $^2A'$	56.6	$SnCl_2$ $^3B_1$	29.4
$ClSn(CH_3)_3$	98.7	$SnCl_3$	43	$ClSnCH_3$ singlet	91.4
$Cl_2Sn(CH_3)_2$	94.8	Cl_2SnCH_3	58.6	$ClSnCH_3$ triplet	51.2
Cl_3SnCH_3	89.2	$ClSn(CH_3)_2$	68.2	SnCl doublet	84.2
		C−H Bonds			
SnH_3CH_3	102.5	$Cl_2Sn(CH_3)_2$	103.3	n-$C_4H_9SnCl_3$	100[a], 102.5[b]
SnH_2CH_3	73	Cl_3SnCH_3	104.1	Cl_2SnCH_3	83.8
		C−C Bonds			
$C_2H_5SnH_3$	87.4	$C_2H_5SnCl_3$	90.3		

[a] $C_4H_9SnCl_3 \leftrightarrow CH_3CH_2CH_2CHSnCl_3 + H$. [b] $C_4H_9SnCl_3 \leftrightarrow CH_2CH_2CH_2CH_2SnCl_3 + H$.

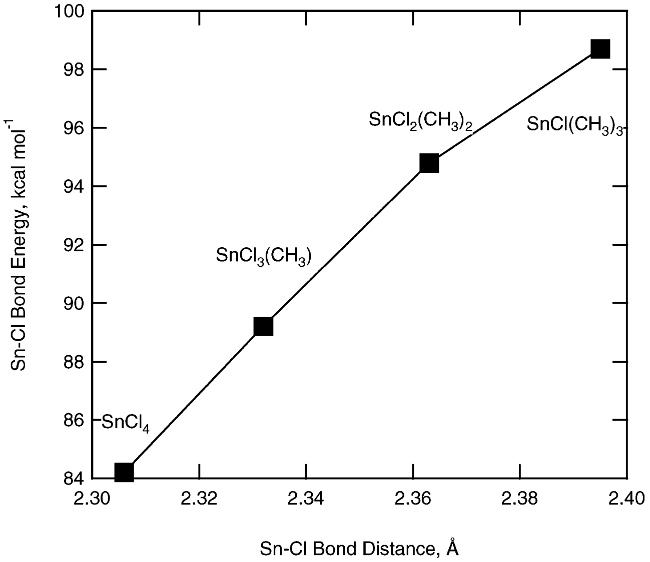

Figure 2. Bond strength (kcal mol^{-1}) vs bond length (Å).

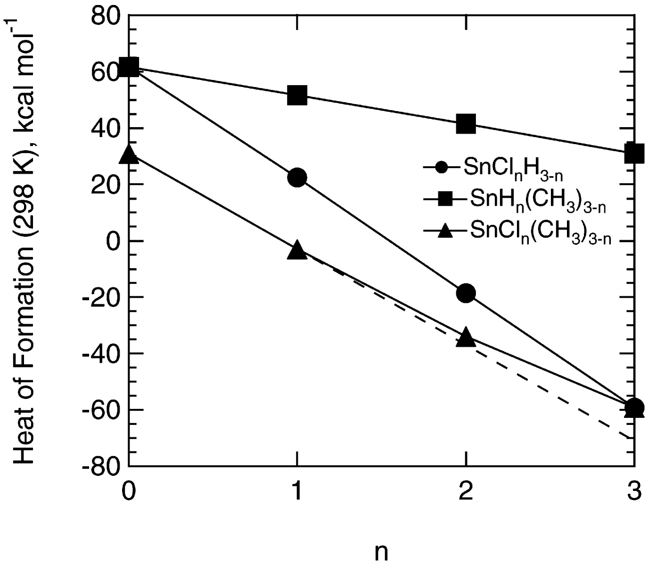

Figure 3. Trends in the heats of formation (298 K) for trivalent species. The dashed line indicates a linear extrapolation of the first two points in the $SnCl_n(CH_3)_{3-n}$ series, highlighting the nonlinearity of the heats of formation.

the BAC-MP4 result. A similar difference is found when the BAC-MP4 result for $(CH_3)Cl_2Sn{-}CH_3$ (69 kcal mol^{-1}) is compared with Price and Trotman-Dickenson's value of 56.1 kcal mol^{-1},[40] again derived from kinetic measurements. As discussed elsewhere,[5] the lower bond energy obtained from the experiment is likely the result of secondary reactions that accelerate the chemistry and yield an activation energy that does not reflect the kinetics of the initial bond fission reaction.

An interesting observation from these calculations is that the predicted Sn−R bond energies do not correlate in the expected manner with bond length (i.e., shorter bonds are not stronger bonds). The most extreme case of this effect is illustrated in Figure 2, which displays bond strength versus bond length data for the $Sn(CH_3)_nCl_{4-n}$ series. In this case, the Sn−Cl bond length increases by ~0.09 Å over the series, whereas the Sn−Cl bond energy increases by nearly 15 kcal mol^{-1}. Similar trends are observable for the Sn−C bond energy in this series, although the magnitude of the effect is weaker. At the opposite extreme, bond lengths in the $Sn(CH_3)_nH_{4-n}$ series are essentially constant, as are the Sn−H bond energies. (The Sn−H bond length varies by <0.015 Å across the series, whereas the Sn−C bond length varies even less; see Table 2.) The SnH_nCl_{4-n} series falls between the two. Such trends are not uniformly observed in other group 14 compounds, although they have been previously predicted for binuclear tin compounds involving substitution by electronegative ligands.[41] Although this effect has not been extensively investigated by computational methods, it is evidently more widespread than would be expected. For example, an examination of previously published geometries for the Si−C−H [9] and Si−C−Cl−H[10] systems shows that, in the analogous silicon series $Si(CH_3)_nCl_{4-n}$, the Si−Cl bonds become longer and stronger with increasing methyl substitution whereas the Si−C bonds become longer and weaker. The reasons for this effect in tin compounds are not fully understood but may involve a combination of factors including polar bonding, negative hyperconjugation (which is evidently a factor in these tin compounds, as discussed above), electronic and nuclear reorganization energies, and hybridization effects (p/s hybridization ratio). Although it is not our intention here to determine which of these is dominant, the results do contribute to the growing body of data challenging the conventional wisdom in which decreasing bond length correlates with increasing bond strength.

Trivalent Molecules. Molecules in the series $Sn(CH_3)_nH_{3-n}$, $SnCl_nH_{3-n}$, and $SnCl_n(CH_3)_{3-n}$ ($n = 0-3$) are all included in this investigation. In all cases, the molecules have pyramidal geometry, with X−Sn−Y bond angles close to tetrahedral. Bond lengths to tin are somewhat longer than those in the tetravalent compounds. With respect to the heats of formation, there are very few experimental data available for comparison. To our knowledge, the only reported heats of formation are for $Sn(CH_3)_3$ (31.1 kcal mol^{-1})[1] and $SnCl_3$ (−69.9 12 kcal mol^{-1}).[2] The BAC-MP4 value for $Sn(CH_3)_3$ is in excellent agreement with the literature value and thus supports the measured Sn−C bond energy on which it is based. In contrast, the agreement with the value reported for $SnCl_3$ is much worse. This is not surprising, however, because the reported heat of formation was derived by comparison with analogous group 14 compounds rather than from a direct measurement, as reflected by the large uncertainty in the number.

The heats of formation in these three molecular series display similar behavior to those in the tetravalent series discussed above. $Sn(CH_3)_nH_{3-n}$ and $SnCl_nH_{3-n}$ show nearly perfect linearity upon substitution of H by CH_3 or Cl, with the heats of formation decreasing by 10.2 and 40.4 kcal mol^{-1}, respectively, for each hydrogen ligand replaced. The replacement of CH_3 by Cl is again nonlinear with respect to the resulting changes in the heat of formation. The first Cl substitution decreases the heat of formation by 34 kcal mol^{-1}, whereas the last decreases it by only 25 kcal mol^{-1}.

Bond strengths in these compounds are, as expected, much weaker than in tetravalent compounds. For example, the Sn−H, Sn−C, and Sn−Cl bond energies in SnH_3, $Sn(CH_3)_3$, and $SnCl_3$ are 48.4, 40.1, and 43 kcal mol^{-1}, respectively, 30−40 kcal mol^{-1} below those in the analogous tetravalent compounds. These smaller bond energies result from the divalent stabilization effect in which the successive removal of ligands from a tetravalent molecule leads to a high−low−high trend in the bond energies. The stabilization of the divalent state is sometimes called the inert pair effect,[42] and its magnitude can be quantified by calculating the exothermicity of the disproportionation reaction

$$2SnX_3 \rightarrow SnX_4 + SnX_2$$

At the BAC-MP4 level of theory, the exothermicities for this reaction for X = H, CH_3, and Cl are −26.5, −30.7, and −41.2 kcal mol^{-1}, respectively. These values are similar to those we predict using BAC-MP4 thermochemistry[9,10] for the analogous silicon reactions (−21.8, −29.7, and −42.6 kcal mol^{-1} for SiH_3, $Si(CH_3)_3$, and $SiCl_3$, respectively). Thus, despite its distance from silicon in the periodic table, tin compounds nevertheless display bonding features that are qualitatively quite similar to those of its other group 14 relatives, a fact that is useful in developing a picture of the overall reactivity of these compounds.

Divalent Molecules. Stanylenes are the analogues of silylenes (SiXY compounds) in that their ground states are all singlets. The energy difference between the singlet ground state and the triplet excited state is large, ranging from about 25 kcal mol^{-1} in SnH_2 to nearly 62 kcal mol^{-1} in $SnCl_2$. Our results for both the singlet−triplet splitting and geometry of SnH_2 are in good agreement with previous calculations in the literature;[43,44] we are unaware of any experimental measurements of this splitting. The variation of the energy splitting as a function of the electronegativity of the ligands is fully consistent with the one observed for the analogous silicon compounds. In silicon compounds, the singlet−triplet splitting also correlates with the reactivity toward insertion into H_2.[11,45] The greater the singlet−triplet splitting, the less reactive the species with respect to bond insertion reactions. Unfortunately, there are no experimental data available to determine the validity of this prediction for tin compounds. Geometrically, stanylenes have longer bond lengths than the tetravalent and trivalent compounds. For example, the Sn−Cl bond length predicted for $SnCl_2$ is 2.396 Å, compared with the experimental value of 2.342 Å obtained from electron diffraction measurements (used by Gurvich et al. to calculate thermochemical properties[2]). Their structures are bent because of the lone pair on the tin atom (the valence shell electron-pair repulsion concept), with tight X−Sn−Y bond angles (91.9, 93.9, and 98.0° in SnH_2, $Sn(CH_3)_2$, and $SnCl_2$, respectively), indicating a relatively low degree of sp^2 hybridization. These geometries are similar to those of the analogous silicon compounds in which the bond angles are 93.3, 98.3, and 101.4° for SiH_2, $Si(CH_3)_2$, and $SiCl_2$, respectively.

As in the case of the other classes of unsaturated tin compounds discussed here, thermodynamic data are scarce. The only heat of formation in the literature for a divalent compound is −48.4 1.7 kcal mol^{-1} for $SnCl_2$, which agrees well with the BAC-MP4 prediction of −45.2 2.2 kcal mol^{-1}. In this case, the condensed phase of the molecule is a stable compound, allowing for relatively straightforward physical characterization and thus higher confidence in the accuracy of the measured value. None of the other divalent tin species reported here have been detected as far as we are aware.

Following the high−low−high trend in bond energies discussed above, the bonds in divalent tin species are predicted to be considerably stronger than those in the trivalent compounds, in some cases exceeding the strength of the same bond in the tetravalent species. For example, in SnH_2, $Sn(CH_3)_2$, and $SnCl_2$, the Sn−X bond energies are 62.5, 56.8, and 91.0 kcal mol^{-1}, respectively. By comparison, the same bond energies in SnH_4, $Sn(CH_3)_4$, and $SnCl_4$ are 74.9, 70.8, and 84.2 kcal mol^{-1}, respectively. The Sn−X bond energies do not change significantly in SnXY compounds, as seen in Table 5.

X_mSnCH_n (m, n = 0−3; x = H or Cl). Selected species within this series were examined as part of this investigation. Their significance derives in part from interest in the gas-phase pyrolysis reactions of organotin precursors used in the CVD of tin oxide. Because these molecules are essentially unknown (no thermodynamic data are available for any of the molecules in this series), a brief examination of the predicted structures for some of these compounds is of interest. In general, the Sn−C bond length decreases as H atoms are removed from the C atom and increases when either H or Cl is removed from Sn (Table 2). This effect is illustrated by the series H_mSnCH_3 (m = 1−3) in which the Sn−C bond length increases from 1.718 Å in H_3SnCH_3 to 2.210 Å in singlet $HSnCH_3$, whereas it decreases to 2.113 Å in triplet *trans*-H_3SnCH. Bond energies follow trends consistent with the stability of the products formed upon removal of a particular ligand. For example, the Sn−C bond energies in H_3SnCH_3, H_2SnCH_3, and $HSnCH_3$ are 68.3, 41.2, and 55.9 kcal mol^{-1}, respectively. The high−low−high pattern already discussed is evident here, indicating the relative stability of the divalent compound.

Ethylene analogue H_2SnCH_2 is predicted to have planar geometry at the HF/6-31G(d) level, in contrast to the most-stable geometry predicted for Sn_2H_4, which is a hydrogen-bridged molecule with a trans structure.[46] The Sn−C bond in this molecule (1.946 Å) is significantly shorter than in its fully saturated counterpart SnH_3CH_3 (2.161 Å). This shorter bond distance coincides with a Sn−C bond energy of 78.2 kcal mol^{-1}, nearly 10 kcal mol^{-1} stronger than in SnH_3CH_3. Sn−H and C−H bond energies in the H_nSnCH_m compounds highlight the stability of the ethylene analogue. For example, the Sn−H bond energy in SnH_3CH_3 is 75.5 kcal mol^{-1}, whereas in SnH_3CH_2 it is only 17.9 kcal mol^{-1}. Similarly, the C−H bond energy in

SnH_3CH_3 is 102.5 kcal mol^{-1}, whereas in SnH_2CH_3 it is only 73 kcal mol^{-1}. Thus, unsaturated organotin compounds have some of the same qualitative bonding features as their lighter-weight group 14 counterparts higher in the periodic table, suggesting a substantial degree of multiple bonding in planar H_2SnCH_2. In contrast with H_2SnCH_2, the geometry of Cl_2SnCH_2 is predicted to have a chair form, with a Sn−C bond length of 2.028 Å. Although this distance is considerably shorter than that in Cl_3SnCH_3 (2.131 Å), the Sn−C bond energy of 49.8 kcal mol^{-1} is 20 kcal mol^{-1} weaker than in Cl_3SnCH_3, evidently because of the much greater stability of $SnCl_2$ relative to SnH_2.

IV. Summary and Conclusions

Ab initio calculations of electronic structure were combined with empirical corrections using a modified BAC-MP4 method to obtain a self-consistent set of thermodynamic data for molecules in the Sn−H−C−Cl system. The electronic structure of the tin atom was modeled using a small-core effective core potential. Although reliable experimental data for comparison with these calculations are available for only a few molecules, the predicted heats of formation are generally in good agreement with these values. Ligand substitution yields trends in the heats of formation that are well reproduced by these calculations. In particular, the highly linear behavior exhibited by the heats of formation in the $Sn(CH_3)_nH_{4-n}$ ($n = 1-4$) series and the nonlinear behavior of the $Sn(CH_3)_nCl_{4-n}$ ($n = 1-4$) series are both reproduced by the BAC-MP4 method. In addition, many features of the bonding observed in analogous group 14 compounds higher in the periodic table, such as those of silicon,[9,10] are also predicted for these compounds. In particular, the high−low−high trend in the bond energies that results from successive ligand removal from SnX_4 species; the stability of X_2SnCH_2 species (X = H or Cl), which are the tin analogues of ethylene; and the trends in the heats of formation just mentioned are all observed. This suggests that, whereas the larger covalent radii are certainly a factor in the bonding of tin compounds, the molecular-orbital properties that determine bonding in other group 14 compounds are consistently present throughout the group, allowing chemical intuition built up through familiarity with compounds of the lighter elements to guide research concerning, for example, chemical reactivity in the heavier analogues. (Note that previous theoretical work on tin compounds indicates that d orbitals play very little role in their bonding.[3]) These consistencies build confidence in the theoretical methods used and suggest that, at least for this class of compounds, high levels of theory and/or larger basis sets are unnecessary to obtain electronic energies of sufficient accuracy to generate thermodynamic data for chemical modeling purposes. Nevertheless, these results also provide challenges to standard expectations, such as the notion that shorter bonds are stronger bonds, highlighting the need to exercise caution when applying generalizations based on analogous chemical systems.

Acknowledgment. We are grateful to Dr. I. M. B. Nielsen for insightful technical discussions during the preparation of this manuscript. Funding for this work was provided by the U.S. Department of Energy Industrial Technologies Program.

Supporting Information Available: Atomic coordinates for each of the molecular species obtained from the HF/6-31G* geometry optimization calculations. Moments of inertia in atomic units (amu Bohr^2) and scaled vibrational frequencies obtained at the same level of theory. Electronic energies resulting from various perturbation-theory calculations using the 6-31G** basis set. The projected UHF (PUHF) and projected UMP2 (PUMP2) energies are given for reference, although they are not used in the derivation of the BACs. Polynomial coefficients (Table S5) for C_p, H, and S as a function of temperature for the species considered in this paper. These fits can be used with the CHEMKIN software package[32] and are defined by

$$\frac{C_p}{R} = a_1 + a_2T + a_3T^2 + a_4T^3 + a_5T^4$$

$$\frac{H}{RT} = a_1 + \frac{a_2}{2}T + \frac{a_3}{3}T^2 + \frac{a_4}{4}T^3 + \frac{a_5}{5}T^4 + \frac{a_6}{T}$$

$$\frac{S}{R} = a_1 \ln T + a_2T + \frac{a_{23}}{2}T^2 + \frac{a_4}{3}T^3 + \frac{a_5}{4}T^4 + a_7$$

References and Notes

(1) Simoes, J. A. M.; Liebman, J. F.; Slayden, S. W. Thermochemistry of Organometallic Compounds of Germanium, Tin, and Lead. In *The Chemistry of Organic Germanium, Tin, and Lead Compounds*; Patai, S., Ed.; Wiley: New York, 1995; p 245.

(2) Gurvich, L. V.; Veyts, I. V.; Alcock, C. B. *Thermodynamic Properties of Individual Substances*; CRC Press: Boca Raton, FL, 1994; Vol. 3.

(3) Karni, M.; Apeloig, Y. Theoretical Aspects of Compounds Containing Si, Ge, Sn and Pb. In *The Chemistry of Organic Silicon Compounds*; Rappoport, Z., Apeloig, Y., Eds.; Wiley: Chichester, U.K., 2001; Vol. 3, p 1.

(4) Basch, H.; Hoz, T. The Nature of the C−M Bond (M = Ge, Sn, Pb). In *The Chemistry of Organic Gemanium, Tin, and Lead Compounds*; Patai, S., Ed.; Wiley: New York, 1995; p 1.

(5) Allendorf, M. D.; Mol, A. M. B. v. *Topics Organomet. Chem.* **2005**, in press.

(6) Allendorf, M. D.; Nielsen, I. M. B.; Melius, C. F.; Mol, A. M. B. v. In *16th Int. Symp. Chem. Vapor Dep./EUROCVD-14*; M. D. Allendorf, F. M., F. Teyssandier, Eds.; The Electrochemical Society Proceedings Series: Pennington, 2003; Vol. PV2003-8; p 55.

(7) Nielsen, I. M. B.; Janssen, C. L.; Allendorf, M. D. *J. Phys. Chem. A* **2002**, *107*, 5122.

(8) Allendorf, M. D.; Melius, C. F. *J. Phys. Chem. A* **1997**, *101*, 2670.

(9) Allendorf, M. D.; Melius, C. F. *J. Phys. Chem.* **1992**, *96*, 428.

(10) Allendorf, M. D.; Melius, C. F. *J. Phys. Chem.* **1993**, *97*, 720.

(11) Allendorf, M. D.; Melius, C. F.; Ho, P.; Zachariah, M. R. *J. Phys. Chem.* **1995**, *99*, 15285.

(12) Allendorf, M. D.; Melius, C. F. *J. Phys. Chem. A* **2002**, *106*, 6370.

(13) Ho, P.; Coltrin, M. E.; Binkley, J. S.; Melius, C. F. *J. Phys. Chem.* **1985**, *89*, 4647.

(14) Ho, P.; Coltrin, M. E.; Binkley, J. S.; Melius, C. F. *J. Phys. Chem.* **1986**, *90*, 3399.

(15) Ho, P.; Melius, C. F. *J. Phys. Chem.* **1990**, *94*, 5120.

(16) Ho, P.; Melius, C. F. *J. Phys. Chem.* **1995**, *99*, 2166.

(17) Melius, C. F.; Ho, P. *J. Phys. Chem.* **1991**, *95*, 1410.

(18) Glaude, P. C., HJ.; Pitz, W.J.; Westbrook, C.K.; Gann, R.G. *Proc. Comb. Inst.* **2000**, *28*, 1749.

(19) Berry, R.; Burgess, D.; Nyden, M.; Zachariah, M.; Melius, C.; Schwartz, M. *J. Phys. Chem.* **1996**, *100*, 7405.

(20) Berry, R.; Ehlers, C.; Burgess, D.; Zachariah, M.; Nyden, M.; Schwartz, M. *J. Mol. Struct.: THEOCHEM* **1998**, *422*, 89.

(21) Zachariah, M.; Westmoreland, P.; Burgess, D.; Tsang, W. *J. Phys. Chem.* **1996**, *100*, 8737.

(22) Melius, C. F. Thermochemistry of Hydrocarbon Intermediates in Combustion: Application of the BAC-MP4 Method. In *Chemistry and Physics of Energetic Materials*; Bulusu, S. N., Ed.; Kluwer Academic Publishers: Dorderecht, The Netherlands, 1990; Vol. 309, p 21.

(23) www.ca.sandia.gov/HiTempThermo/index.html.

(24) Frisch, M. J.; Trucks, G. W.; Schlegel, H. B.; Gill, P. M. W.; Johnson, B. G.; Robb, M. A.; Cheeseman, J. R.; Keith, T.; Petersson, G. A.; Montgomery, J. A.; Raghavachari, K.; Al-Laham, M. A.; Zakrzewski, V. G.; Ortiz, J. V.; Foresman, J. B.; Cioslowski, J.; Stefanov, B. B.; Nanayakkara, A.; Challacombe, M.; Peng, C. Y.; Ayala, P. Y.; Chen, W.; Wong, M. W.; Andres, J. L.; Replogle, E. S.; Gomperts, R.; Martin, R. L.; Fox, D. J.; Binkley, J. S.; Defrees, D. J.; Baker, J.; Stewart, J. P.; Head-Gordon, M.; Gonzalez, C.; Pople, J. A. *Gaussian 94*, revision D.3; Gaussian, Inc.: Pittsburgh, PA, 1995.

(25) LaJohn, L. A.; Christiansen, P. A.; Ross, R. B.; Atashroo, T.; Ermler, W. C. *J. Chem. Phys.* **1987**, *87*, 2812.

(26) Basis sets were obtained from the *Extensible Computational Chemistry Environment Basis Set Database*, version 12/03/03, as developed and distributed by the Molecular Science Computing Facility, Environmental and Molecular Sciences Laboratory, which is part of the Pacific Northwest Laboratory, P.O. Box 999, Richland, WA 99352, and is funded by the U.S. Department of Energy. The Pacific Northwest Laboratory is a multi-program laboratory operated by Battelle Memorial Institute for the U.S. Department of Energy under contract DE-AC06-76RLO 1830. Contact David Feller or Karen Schuchardt for further information.

(27) Wagman, D. D.; Evans, W. H.; Parker, V. B.; Schumm, R. H.; Halow, I.; Bailey, S. M.; Churney, K. L.; Nuttall, R. L. *J. Phys. Chem. Ref. Data* **1982**, *11*, *Suppl. 2*.

(28) Chase, M. W.; Davies, C. A.; Downey, J. R.; Frurip, D. J.; McDonald, R. A.; Szverud, A. N. *J. Phys. Chem. Ref. Data* **1985**, *1985*, 14.

(29) We recently determined that these corrections were not fully implemented in published BAC-MP4 and BAC-G2 data (refs 8−12, 16, 17). Typically, the values of $S°(298)$ fully corrected for hindered rotors differs by less than 1 cal mol^{-1} K^{-1} from the published value. Similarly, $\Delta G°_f$ differs by less than 2 kcal mol^{-1} at 1500 K. (The difference in the free energy is magnified by increasing temperature.) In some cases, larger differences are observed, particularly for molecules containing several rotors. Thermodynamic data (including polynomial fits) that are fully corrected for hindered rotors are now posted on the web site www.ca.sandia.gov/HiTempThermo/index.html, which provides a table of $S°(T)$ and $\Delta G°_f(T)$ for comparison with earlier values given in the references cited above.

(30) Pitzer, K. S.; Gwinn, W. D. *J. Chem. Phys.* **1942**, *10*, 428.

(31) Benson, S. W. *Thermochemical Kinetics*, 2nd ed.; Wiley: New York, 1976.

(32) Kee, R. J.; Rupley, F. M.; Miller, J. A.; Coltrin, M. E.; Grcar, J. F.; Meeks, E.; Moffat, H. K.; Lutz, A. E.; Dixon-Lewis, G.; Smooke, M. D.; Warnatz, J.; Evans, G. H.; Larson, R. S.; Mitchell, R. E.; Petzold, L. R.; Reynolds, W. C.; Caracotsios, M.; Stewart, W. E.; Glarborg, P.; Wang, C.; Adignun, O. *Chemkin Collection*; release 3.6 ed.; Reaction Design, Inc.: San Diego, CA, 2000.

(33) Mackay, K. M. Structural Aspects of Compounds Containing C−E (E = Ge, Sn, Pb) bonds. In *The Chemistry of Organic Germanium, Tin, and Lead Compounds*; Patai, S., Ed.; Wiley: New York, 1995; p 97.

(34) Hehre, W. J.; Radom, L.; Schleyer, P. v. R.; Pople, J. A. *Ab Initio Molecular Orbital Theory*; Wiley: New York, 1986.

(35) Jonas, V.; Frenking, G.; Reetz, M. T. *J. Comput. Chem.* **1992**, *13*, 935.

(36) Wadt, W. R.; Hay, P. J. *J. Chem. Phys.* **1985**, *82*, 284.

(37) Kaupp, M.; Schleyer, P. v. R. *J. Am. Chem. Soc.* **1993**, *115*, 1061.

(38) Charton, M. Substituent Effects of Germanium, Tin, and Lead Groups. In *The Chemistry of Organic Germanium, Tin, and Lead Compounds*; Patai, S., Ed.; Wiley: New York, 1995; p 603.

(39) Johnson, R. P.; Price, S. J. W. *Can. J. Chem.* **1972**, *50*, 50.

(40) Price, S. J. W.; Trotman-Dickenson, A. F. *Trans. Faraday Soc.* **1958**, *54*, 1630.

(41) Kaupp, M.; Metz, B.; Stoll, H. *Angew. Chem., Int. Ed.* **2000**, *39*, 4607.

(42) Walsh, R. *Acc. Chem. Res.* **1981**, *14*, 246.

(43) Selmani, A.; Salahub, D. R. *J. Chem. Phys.* **1988**, *89*, 1529.

(44) Balasubramanian, K. *J. Chem. Phys.* **1988**, *89*, 5731.

(45) Sosa, C.; Schlegel, H. B. *J. Am. Chem. Soc.* **1984**, *106*, 5847.

(46) Trinquier, G. *J. Am. Chem. Soc.* **1990**, *112*, 2130.

(47) Baldwin, J. C.; Lappert, M. F.; Pedley, J. P.; Poland, J. S. *J. Chem. Soc., Dalton Trans.* **1972**, 1943.

(48) Spalding, T. R. *J. Organomet. Chem.* **1973**, *55*, C65.

(49) Gmelin, L. *Gmelin Handbook of Inorganic and Organometallic Chemistry. System number 46. Sn−Organotin Compounds*; Springer: Berlin, 1975; Vol. 1.